Title

Modeling the Electrocatalytic Interface in the Conditions of Electrochemical Amination of Acetone with Methylamine as Nitrogen Source

Author

Guan, Yani

Publication Date

2024

Peer reviewed|Thesis/dissertation

UNIVERSITY OF CALIFORNIA
Los Angeles

Modeling the Electrocatalytic Interface in the Conditions of Electrochemical Amination of Acetone with Methylamine as Nitrogen Source

A thesis submitted in partial satisfaction
of the requirements for the degree
Master of Science in Chemical Engineering

by

Yani Guan

2024

ABSTRACT OF THE THESIS

Modeling the Electrocatalytic Interface
in the Conditions of Electrochemical Amination of Acetone with Methylamine as Nitrogen Source

by

Yani Guan
Master of Science in Chemical Engineering
University of California, Los Angeles, 2024
Professor Philippe Sautet, Chair

Electric double layer on Cu electrode was studied in the conditions of electrochemical amination of acetone with methylamine as Nitrogen source. Double layer capacitance is used as a key descriptor to investigate the surface pre-configuration or preference of adsorption. It was found that in alkaline water solution, acetone (hydrophobic) and methylamine (hydrophilic) will result in different local dielectric property, which cause increase/decrease in Helmholtz capacitance.

Besides, it was observed that the working Cu electrode is corroded using mixtures of acetone and methylamine even under reductive potential conditions (-0.75V vs RHE). We employed Grand Canonical density functional theory to understand this dynamic process under potential from a microscopic perspective. We show that amine ligands in solution directly adsorb on the electrode, coordinate with the metal center, drive the rearrangement of the copper surface by extracting Cu atoms in low coordination positions, finally forming a detached Cu-tetramine di-cation complex in solution, even at negative potential conditions.

The thesis of Yani Guan is approved.

Carlos Morales-Guio

Dante A. Simonetti

Panagiotis D. Christofides

Philippe Sautet, Committee Chair

University of California, Los Angeles

2024

Dedicated to my mother

TABLE OF CONTENTS

LIST OF FIGURES

ACKNOWLEDGMENTS

I extend my heartfelt appreciation to Professor Philippe Sautet for his guidance, patience, and invaluable insights throughout the course of this research. His expertise and encouragement have been instrumental in shaping this thesis.

I am grateful to the members of my academic committee, Panagiotis D. Christofides, Dante A. Simonetti and Carlos Morales-Guio, for their constructive feedback and suggestions, which have enriched the quality of this work.

I would like to thank my parents for their unwavering support, understanding, and encouragement. Their love and belief in me have been my greatest source of strength.

I am indebted to Ziyu for her encouragement, motivation, and accompany during the ups and downs of this journey.

I extend my gratitude to current and former members of Professor Sautet's group, particularly Dr. Simran Kumari, Dongfang Cheng, Yichen Li, Ziqi Jiang and Bobby Kowalski. Besides, thanks for my collaborators Justus Kumper and Professor Regina Palkovits at RWTH Aachen University.

I acknowledge UCLA for providing the necessary resources and facilities for conducting this research, specifically the UCLA Institute for Digital Research and Education (IDRE) and the computational resources on the Hoffman2 cluster. I also thank the computational resources on the Bridges2 and Expanse cluster from the ACCESS program.

This thesis contains materials from unpublished manuscripts.

CHAPTER 1

Introduction

1.1 Electrochemical Amination

Electrochemical reduction[1, 2] is a fundamental process in electrochemistry where a chemical species gains electrons, resulting in a decrease in its oxidation state or an increase in its electron density. This reduction occurs at the cathode, the electrode where reduction reactions take place, in an electrochemical cell. Electrochemical reduction plays a crucial role in various fields, including energy storage, chemical synthesis, environmental remediation, and analytical chemistry[3, 4].

In electrochemical reduction, the cathode serves as the site for electron transfer reactions. When an external electrical potential is applied across the electrodes immersed in an electrolyte solution, electrons flow from the anode (where oxidation occurs) to the cathode (where reduction occurs). At the cathode, the electrons are gained by the species undergoing reduction, leading to its transformation into a reduced form.

Electrochemical amination of ketones[5, 6, 7] (Figure 1.1) involves the introduction of amino groups into ketone molecules using electrochemical methods. This process provides a direct and efficient route to access amines from readily available starting materials. In cathodic Electrochemical amination, cathodic electrochemical amination relies on the reduction of a nitrogen-containing species at the cathode, generating reactive nitrogen radicals or anions. These species then react with the ketone substrate, resulting in the formation of the corresponding amine product.

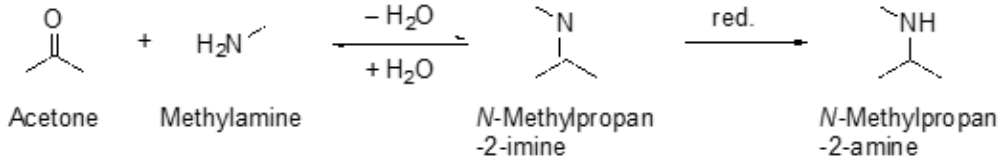

Figure 1.1: The equilibrium reaction of acetone and methylamine is a condensation and yields N-methyl-propan-2-imine. The imine can be reduced and results in N-methyl-propan-2-amine.

1.2 Cu Electrode

Copper (Cu) has emerged as a pivotal catalyst in the realm of electrochemical amination, standing as a cornerstone for the efficient and selective transformation of organic substrates into valuable amine derivatives[7, 8, 9]. This catalyst exhibits remarkable versatility as a catalytic species in electrochemical transformations. Its ability to mediate a broad range of redox reactions, coupled with its facile interconversion between different oxidation states, renders it well-suited for catalyzing diverse amination processes. Copper catalysts often demonstrate high catalytic activity in electrochemical amination reactions, enabling efficient nitrogen incorporation into organic substrates such as ketones, aldehydes, and olefins. This high activity translates into enhanced reaction rates and improved overall synthetic efficiency.

The redox-active nature of copper facilitates facile redox cycling between its different oxidation states (Cu^0, Cu^+, Cu^{2+}), enabling it to participate readily in electron transfer processes during electrochemical reactions[10, 11]. This inherent redox flexibility contributes to the catalytic turnover and longevity of copper catalysts.

1.3 Electric Double Layer

The electric double layer (EDL) stands as a pivotal concept in electrochemistry, encapsulating the intricate interplay between charged surfaces and electrolyte solutions at the

nanoscale. This introduction delves into the fundamental principles underlying the electric double layer phenomenon, elucidating its structural characteristics, dynamic behavior, and diverse applications across scientific disciplines. By exploring the foundational aspects of the electric double layer, we unveil its significance in elucidating electrochemical phenomena, engineering functional materials, and advancing technologies ranging from energy storage to biosensing.

At the interface between an electrode and an electrolyte solution, charges accumulate due to the presence of oppositely charged species. This accumulation leads to the formation of a diffuse layer of counterions near the electrode surface, balancing the surface charge and establishing electroneutrality. The Gouy-Chapman model provides a theoretical framework for describing the distribution of ions in the electric double layer as shown in Figure 1.2. It posits that the distribution of ions follows an exponential decay profile, with the concentration of ions decreasing exponentially with distance from the charged surface.

The capacitance of the electric double layer, known as double layer capacitance, reflects the ability of the interface to store charge in response to an applied potential. It plays a crucial role in electrochemical impedance spectroscopy, energy storage devices, and electrochemical sensing platforms.

1.4 Electrode Dissolution

Electrode dissolution under methylamine represents a fascinating and intricate phenomenon within the realm of electrochemistry, characterized by the intricate interplay between the electrode surface, the methylamine species, and the surrounding electrolyte environment. At the interface between the electrode surface and the methylamine-containing electrolyte, electrochemical reactions occur, leading to the dissolution of the electrode material. These reactions involve the exchange of electrons and ions between the electrode and the electrolyte, resulting in changes to the electrode's surface morphology and composition.

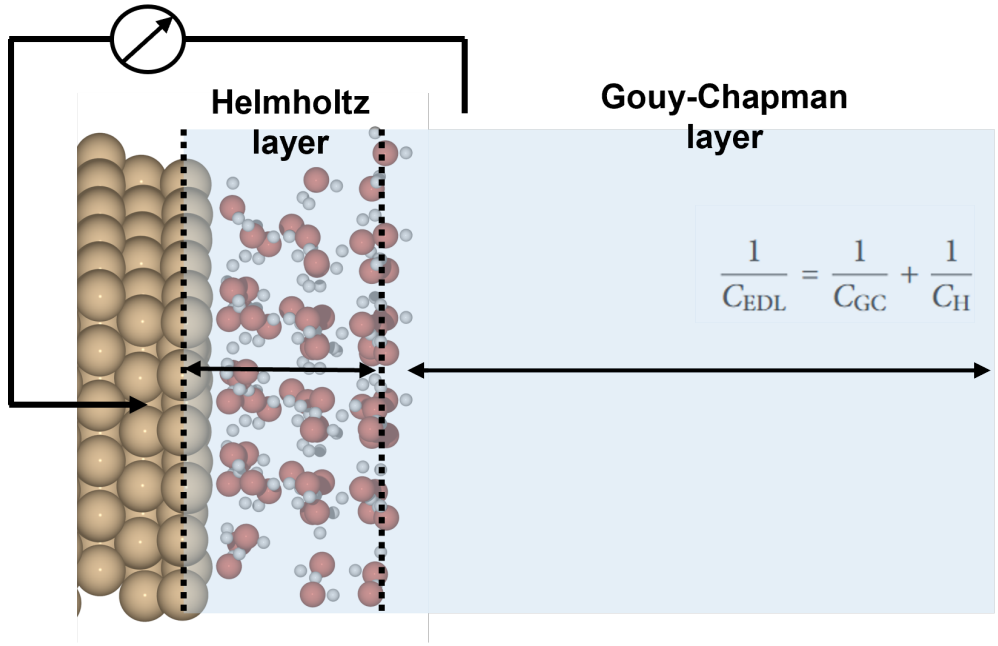

Figure 1.2: Atomistic model of Cu(111)/electrolyte interface

Methylamine, a primary aliphatic amine, can undergo various chemical transformations under electrochemical conditions, including protonation, deprotonation, and redox reactions. These speciation changes influence its reactivity towards the electrode surface and modulate the dissolution process. Methylamine, in its protonated form (e.g., methylammonium cation), can act as a corrosive agent, promoting the dissolution of certain electrode materials through chemical reactions such as metal oxidation and dissolution. The presence of methylamine-derived species enhances the dissolution kinetics and alters the electrochemical stability of the electrode surface.

1.5 Density Functional Theory

Density Functional Theory (DFT) stands as a cornerstone in computational quantum chemistry, offering a powerful framework for predicting and understanding the electronic structure and properties of atoms, molecules, and condensed matter systems. At its core,

DFT revolves around the concept of the electron density—a fundamental property that encapsulates the distribution of electrons within a system. Rather than directly solving the many-body Schrödinger equation, DFT seeks to minimize the total electronic energy functional, which is expressed in terms of the electron density. Through this approach, DFT provides a tractable yet accurate means of approximating the ground-state properties of complex systems, including molecular geometries, electronic energies, reaction pathways, and spectroscopic properties. Its versatility and computational efficiency have made DFT an indispensable tool in a wide range of scientific disciplines, spanning chemistry, physics, materials science, and beyond. Despite its remarkable success, challenges persist in developing more accurate exchange-correlation functionals and addressing the treatment of strongly correlated systems. Nevertheless, the continued refinement and application of DFT promise to unlock new insights into the behavior of matter at the atomic and molecular scales, driving forward advances in both fundamental understanding and technological innovation.

CHAPTER 2

Electric Double Layer Capacitance

2.1 Background in Literature on Modelling of Interface

The Poisson-Boltzmann and GCS theories, commonly used to describe the electrical double layer, fall short due to their simplified assumptions about ions and solvent molecules. Boda et al.[12] and Moraila-Martínez et al.[13] found discrepancies between these theories and actual observations, highlighting the need for advanced experimental and theoretical methods, especially in electrochemistry and biophysics, where precise ion-surface interactions are crucial.

Empirical adsorption models, developed over 40 years ago, have been essential in designing and optimizing ion exchange chromatography (IEC) processes for proteins. However, transferring knowledge between systems has been limited. To address this, Essert et al.[14] investigated the physicochemical adsorption mechanism in IEC, developing a quantitative method to measure the effective electrical double layer (EDL) thickness. Their findings shed light on the factors influencing EDL expansion and offer insights into optimizing resin design and biomolecule purification processes in IEC, potentially addressing technological and economic challenges.

2.2 Introduction

Biomass, e.g. levulinic acid, presents a promising renewable carbon source bearing the potential to create closed carbon cycles, which is beneficial for the depletion of fossil resources[15, 16, 17]. Electrochemical amination of levulinic acid offers the chance to selectively introduce nitrogen functionalities into organic compounds, showing a promising industry application. At the same time, solid-liquid interfaces are omnipresent in nature, and it is thought that chemical reactions involving electron transfer and bond breaking/forming take place inside the electric double layers. A mechanistic understanding of interfacial phenomena during electrosynthesis within electric double layer is therefore important.

Based on Stern theory, electric double layer (EDL) consists of long range Gouy–Chapman layers and a short range Helmholtz layer between the electronically conducting electrodes and the ionically conducting electrolytes[18, 19]. The applied potential controls the strength of the electric field and the surface charge density, which have a profound impact on the electrocatalytic reactions. Furthermore, there is ample evidence in the literature that the microscopic structures of interface water and solvated ions in the EDL can significantly alter the electrocatalytic activity of electrode materials. Therefore, it is vital to elucidate the EDL structures and the dielectric properties (i.e., the capacitance) at the atomic level to improve our understanding of electrocatalysis as well as to distinguish between true on electrode and close to electrode surfaces reaction processes. However, electrostatic interactions at solid-liquid interfaces are drastically modified due to the most salient properties of water – its polarity. This has profound implications for the behavior of adsorption. As a result, understanding the structural and dynamical properties of the organic reactant and the interfacial water molecules is of vital importance[20, 21].

This understanding of dielectric properties of SLI paves the way for a complete picture of the molecular configurations close to or at the electrode surface in the presence of an electrochemical potential[20, 19]. In the context of probing actual electrode configurations,

impedance spectroscopy measurements can provide exact double layer capacitance to investigate the adsorption of organic molecules. As organic molecules adsorb most strongly at the potential of zero charge (E_{pzc}) (minimal competition with the adsorption of ions), adsorption investigations of uncharged organic molecules are usually done at that potential. However, the knowledge of the change in double layer capacitance obtained from the impedance spectroscopy measurements does not provide any conclusions about which effect or which realistic geometrical configuration of the organic molecules on the electrode surface or close to it causes the observed change.

Here, we address how organic molecules can change the EDL capacitance and how the configuration of the molecule at or near the copper electrode surface controls these changes. Acetone and methylamine were selected as model compounds rather than using longer-chain ketones or primary amines to present important reactants during electrochemical amination as they are the first representatives of their homologous series. Aiming at decoding Helmholtz capacitance at E_{pzc}, this works starts from copper/water interface, water molecules' dielectric effects (i.e., the influence on capacitance) are studied via GCDFT. At the same time, AIMD analysis of dynamic capacitance profile is used to fully include the effects of re-orientation of water molecules. On the next, based on the molecular characteristics of acetone/methylamine, for example, the polarity of molecules, 2.88 D (acetone) vs 1.31 D (methylamine), their mixtures with water are constructed to represent the actual interactions to the most degree. Corresponding stability and capacitance diagrams are obtained to analysis thermal stability and electrochemical performance of interfaces while sampling analysis of capacitance fully consider the steric effects of adsorbates. At the same time, impedance spectroscopy measurements were applied to probe the capacitance at E_{pzc} of the EDL forming at different concentrations in aqueous environment. For further analysis, isothermal adsorption curves were obtained using capacitance compared with that at saturation coverage to study the adsorption behaviors.

Our aim is therefore to share a better understanding of the environment of a copper

electrode in the presence of uncharged organic molecules at the potential of zero charge in aqueous solutions, based on the double layer capacitance.

2.3 Methods

2.3.1 GCDFT Simulations of Solvated Models on Cu (111)

The free energy was evaluated by grand canonical density functional theory (GCDFT) calculations, which is a surface charging technique. Details can be found in our previous work[11, 22, 23, 24], and here we summarize the key points with respect to the Helmholtz capacitance,

$\Omega(U) = E(U) - q(U)FU = E_0 - \frac{1}{2}C(U - U_0)^2$

which treats the electrochemical interface as an effective capacitor. Here, E(U) is the electronic energy of the surface under a potential U, which is calculated by referencing the Fermi level of the system against the vacuum level. q(U) is the surface charge difference referenced against the neutral system, and F is the Faraday constant. U_0 stands for the potential of zero charge in the vacuum scale, and C is the effective capacitance. The self-consistent implicit solvation model VASPsol was used to represent the polarizable electrolyte region[25]. The surface slab was symmetrized along z axis to avoid a global electric dipole and an asymmetrical potential in the implicit solvation region.

The surface free energy was calculated based on the grand canonical free energy to study their stability at PZC.

$\Delta G = G_{system} - G_{slab} - n_1 * [E_{water} - \frac{1}{2}T(S_{trans} + S_{rot})] - n_2 * [E_{acetone/methylamine} - \frac{1}{2}T(S_{trans} + S_{rot})]$

The translational and rotational entropy of liquid water and adsorbates in solvation is approximated as half the value for the ideal gas phase.

2.3.2 AIMD Sampling of Thermal Fluctuations within Solvated Models

Ab initio molecular dynamics simulations were performed using the VASP program. Optimized structures with the same DFT setting were selected as initial configurations. AIMD simulations were initially run in the NVT canonical ensemble at a temperature of 400K, and the time step was set to 1.2 fs. Trajectories of around 10ps (10000 steps) were collected. After that, NVT canonical ensemble at room temperature was used to obtain another 10ps trajectory after the high temperature exploring of the system . From those simulation of 10,000 steps, a point is collected every 200 steps during the second 5,000 steps to calculate their averaged Helmholtz capacitance using GCDFT.

2.4 Results and Discussion

2.4.1 Cu/Water Interface

Calculations show that on the low-index Cu (111) surface, the copper-water interaction is rather weak and the distribution of water molecules in the first hydration shell exhibits a double layer structure with molecules that are closest to surface located on top of the Cu sites. The atomistic model of the Cu (111)/water interface is shown in Figure 1.2. Starting from those insights from literature, water models are constructed layer by layer to enable full equilibrium between each layer, and combined with an implicit solvation model, with a dielectric constant of 78.4, to represent the influence of the rest of the bulk water. Static geometry optimization calculations, considered as a first rough approach, show that, as the number of water layer increases from one to four, there is a decrease in Helmholtz capacitance but an increase in adsorption free energy per unit surface area Figure 2.2. This adsorption free energy is clearly proportional to the number of layers, while the value normalized by the number of water layer is quasi-constant and converges after three layers. In order to balance accuracy and efficiency, we will consider three water layers in this work to represent the Cu

(111)/water interface.

To be specific, the capacitance for the three-water layer model is around 8.5 $\mu F/\mathrm{cm}^2$. Static calculations are however not sufficient, as fluctuations in the orientation of water molecules will influence the surface dipole significantly, which will change the surface electronic structure, for example the charge transfer, electrostatic potential, local electric field, etc.. Therefore, AIMD calculations were considered in order to first equilibrate the water structures and then to calculate an average capacitance value along the trajectory, by taking one snapshot every 200 points, first at 400 K then at room temperature. Figure 2.3 gives the dynamic profile of the capacitance of the three-water layer model. The average value is only slight modified compared to static value (8.44 $\mu F/\mathrm{cm}^2$ at 400 K and 8.23 $\mu F/\mathrm{cm}^2$ at 300 K). Compared with the capacitance of the bare Cu surface in the implicit water solvent (26.7 $\mu F/\mathrm{cm}^2$, Figure 2.1), the presence of explicit water adsorbates clearly reduces the capacitance at the PZC by a factor of about 3. With regard to this decrease in capacitance, Stern proposed a model for an aqueous interface where the dielectric constant is reduced over a nanoscopic width. Following the Stern's electric double layer model, the decrease of the interfacial capacitance for a dipolar fluid has been related to molecular ordering and orientation using approximate statistical mechanical methods. Besides, Bonthuis et al studied both parallel and perpendicular interfacial dielectric response functions of aqueous interface and demonstrated that the perpendicular dielectric function exhibits singularities like the nonlocal bulk dielectric function, indicating anomalous screening effects at the interface.

Noted that tuning electron numbers of system, not only will the electrode surface respond to, but also the mixture part seems to be able to hold charge. It is in line with the work from Cheng et al that the Helmholtz capacitance is divided into two parts in series: the one that is due to the usual dielectric response of the solvent in the Helmholtz layer (C_{sol}), and the other accounts for the effect of water chemisorption (C_A). Therefore, the electrochemical interactions within the Helmholtz layer have a lot to do with the capacitance trends.

Note that the Gouy–Chapman layers were not considered in modeled interfaces since

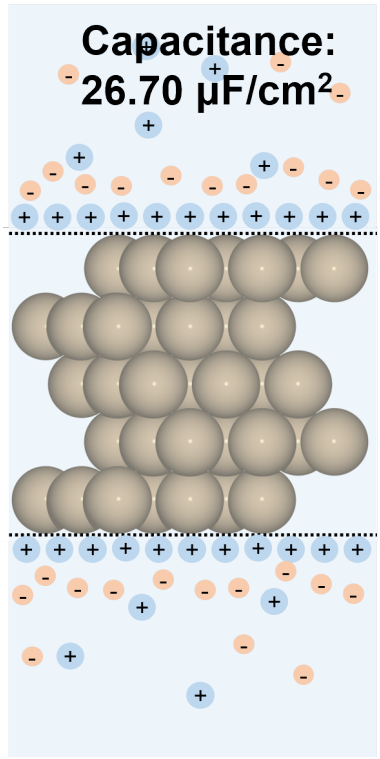

Figure 2.1: The bare Cu (111) surface in a continuum model of the water/$NaClO_4$ electrolyte environment and its calculated capacitance at PZC

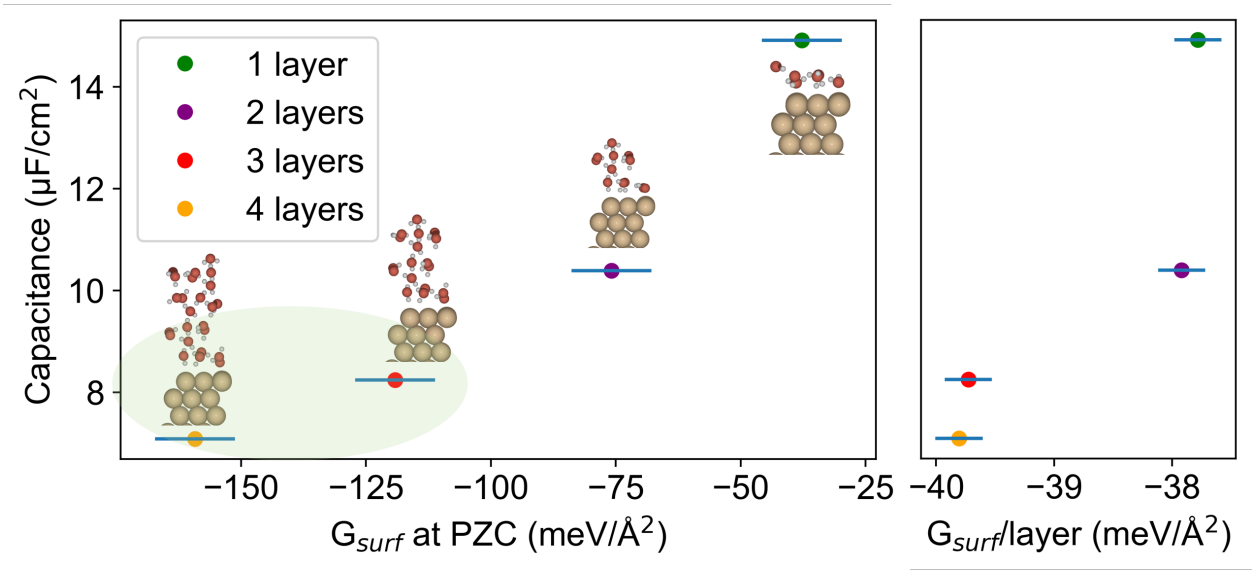

Figure 2.2: Capacitance calculated from the static approach and corresponding adsorption free energy per surface area for different numbers of explicit water layers (1, 2, 3 and 4); on the right the adsorption free energy is normalized per layer

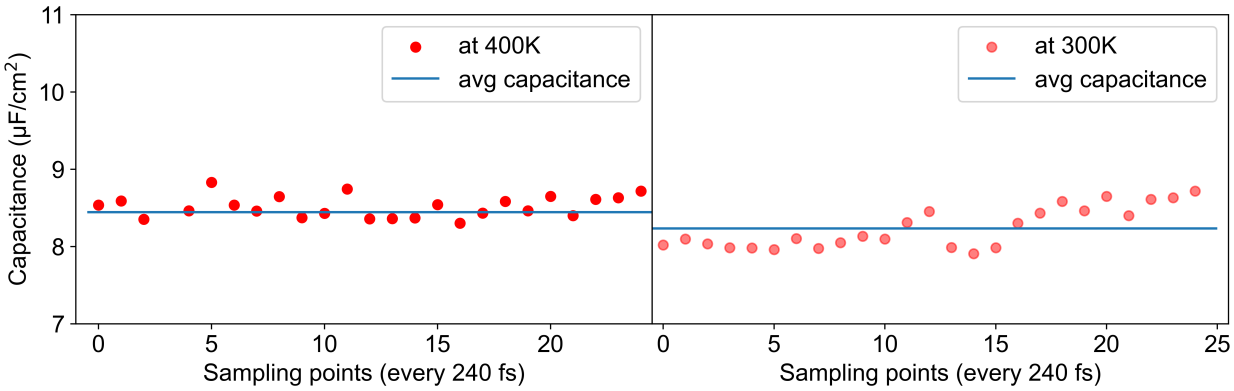

Figure 2.3: Calculated capacitance from AIMD sampling of the Cu(111)/water interface at PZC, including configurations every 200 point along the 10 ps trajectory at 400K (left) and at 300 K(right). The blue line shows the average capacitance value.

the use of electrolyte with relatively high concentration (0.01 M $NaClO_4$) and polar solvents in typical experimental setup maximizes the Gouy–Chapman contribution to the capacitance C_{GC}, and thus, surface charges are effectively screened within the Helmholtz layers. Therefore, the capacitance of the electric double layer is controlled by the Helmholtz layer contribution C_H corresponding to the zone near the electrode surface.

2.4.2 Dielectric Properties within the Helmholtz Layer including Adsorbates

Modeling adsorption at metal/water interfaces is a cornerstone toward an improved understanding of heterogeneous electrocatalysis. An hybrid scheme was used to describe specific interactions near the surface between water and acetone using explicit solvation model. Molecular characteristics in polar aqueous environment of acetone and methylamine are considered to construct solvated models to represent the actual interfacial phenomenon to the most degree.

2.4.2.1 Acetone

Acetone is considered as a hydrophobic molecule. Even in basic conditions, acetone, being a neutral organic compound, does not have any ionizable groups that can directly interact with or be affected by changes in pH. Such a hydrophobic nature can be considered as a structure breaker that is expected to result in a water depletion layer (also called hydrophobic gap). It is confirmed by some experiment and theoretical simulations work that the dielectric medium inside the Helmholtz layer may be not homogeneous like that represented in the traditional model.

Starting from above insights, two acetone molecules were used to occupy each water layer in our three water layer surface model as shown in Figure 2.4 (a). In Figure 2.4 (b), the adsorption free energy per unit surface area ($Å^2$) is decreased in absolute value from around 120 meV (three water layers) to 85 95 meV (one acetone layer and two water layers).

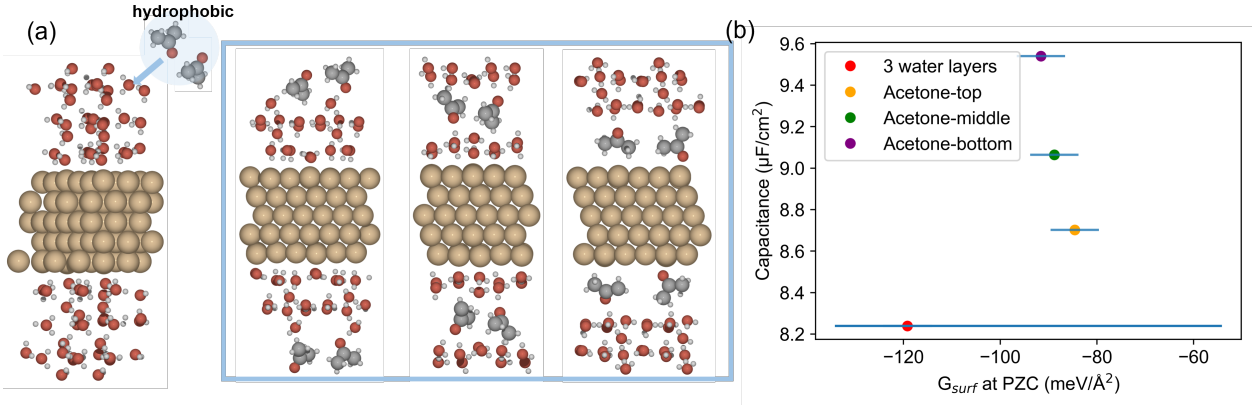

Figure 2.4: (a) Diagram of mixture models where acetone is in the top layer, middle layer and bottom layer as hydrophobic gap; (b) capacitance calculated from the static approach and corresponding adsorption free energy per surface area for those models

It is intuitive that the depletion layer, as a structure breaker, results in a destabilization of the surface in aqueous environment due to the reduced number of hydrogen bonds. The capacitance significantly increases compared with the three water layer model in the absence of acetone. This can be explained by the dielectric constant of the gap layer, which is extremely high (with properties close to implicit solvation) and, thus, is important for the total EDL capacitance.

As before, AIMD simulations have been used to model the evolution of the capacitance along a dynamic trajectory (Figure 2.5) with different positions of the acetone molecules in the water layers. All simulations correspond to an increase in the capacitance and the relative value ordering of the capacitance values of those three mixtures model of acetone and water is consistent, but the average value of the capacitance along the dynamic trajectory can slightly higher than the value for the static configuration. In static calculations, the capacitance of mixture models is between around 8.70 and 9.50 while when to AIMD sampling, the average capacitance is between 9.00 and 10.50. This kind of capacitance switch also validates the fact that this hydrophobic molecule naturally will disturb water layers largely and bring out the significant dielectric effects before it reaches equilibrium. When acetone in the

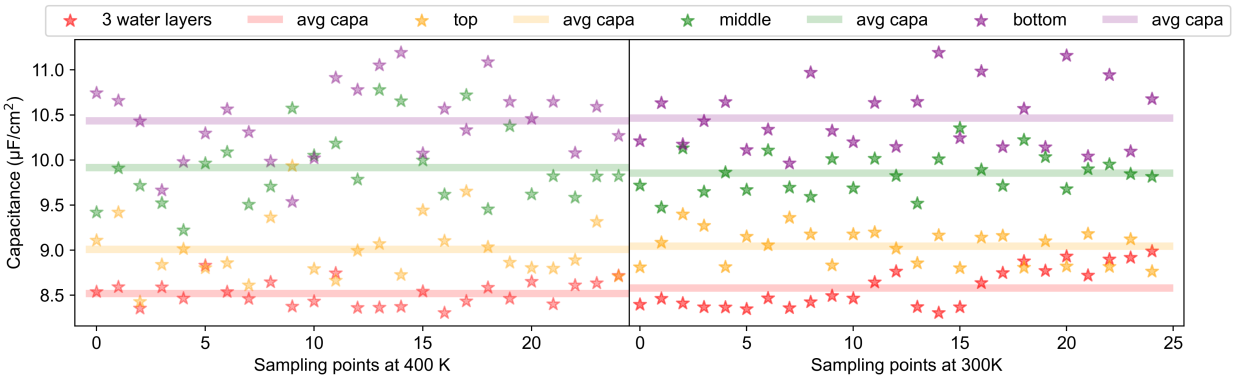

Figure 2.5: AIMD sampling of three water layers and mixture models of acetone and water at 400K (left) and at 300K (right) at PZC including a snapshot every 200 steps during the second 5,000 steps of simulations, where their dynamic capacitance profiles are shown. The horizontal lines represent the average capacitance value.

first (bottom) layer, interacting with the surface and separating water from it, the largest capacitance increase is found. To be specific, at PZC, the bottom water layer's configuration is a combination of H down and O bonded on the electrode surface. As acetone molecules are added dropwise to the system, they will reach the surface of the electrode or a location near the electrode before reaction occurs. When acetone reaches the electrode surface, it will result in the most significant effects of dielectric effects (capacitance increase mostly) since acetone takes up the positions of water molecules that are bonded via O on the surface. Also, the smallest capacitance increase is found when acetone is present in the third layer, between the bulk water and the explicit water layer, since in this configuration acetone only weakly perturbs the water/Cu interfacial Helmholtz layer.

2.4.2.2 Methylamine

When it comes to methyl amine, the amino group (-NH_2) of methylamine (CH_3NH_2), would likely promote the hydrolysis of water, which results in local OH^- anions -NH_3^+ cations increase. It is that methylamine would generally be more hydrophilic due to the presence

of charged groups that can interact favorably with water. It is different from acetone for methylamine that this medium prefers to stay with water and even bring out hydrolysis forming complexes ($CH_3NH_3^+OH^-$). Thus, when it comes to constructing mixture models, the combination of methylamine and water in the same layer is included. It is natural to think about the percentage of water and methylamine. Considering the actual monolayer configurations, typical experimental set-up and actual simulation cell size compared with molecule's size, three methylamine to replace four water molecules was used to represent monolayer methylamine density, and one methylamine to replace two water molecules was used to represent low concentration of methylamine, as well as two methylamine to replace three water molecules to make the first two models are connected and keep in line with acetone's mixture models.

It was exciting to notice that after geometry optimization of those mixture models, methylamine does contribute to hydrolysis of water and form $CH_3NH_3^+OH^-$ complex while when methylamine is in the bottom layer, it either forms $CH_3NH_3^+OH^-$ complex or bonds on the surface. As shown in Figure 2.7 (a), it can be seen as representing low concentration situation and wherever methylamine exists in which layer, they all decrease the capacitance compared with three water layers. It does make sense that the conductive ions existence will reduce the dielectric effect within Helmholtz layer and thus lower the capacitance. It is of great importance to note that as shown in the diagram, when it comes to that configuration with methylamine in the top layer, it doesn't form $CH_3NH_3^+OH^-$ complex completely with N pointing toward one hydrogen in water molecule in a shorter distance. It just lowers the capacitance a little bit that also validates this kind of explanation. The adsorption free energy per unit surface (Figure 2.7 (b)) is very comparable with the reference three-water layer model when methylamine forms complete complex with water molecules. When it comes the model where methylamine is in the top layer with a quasi-formation of complex, meaning the interaction between methylamine and water is not as strong as that from models with complete formation, the adsorption free energy is less than that of reference system.

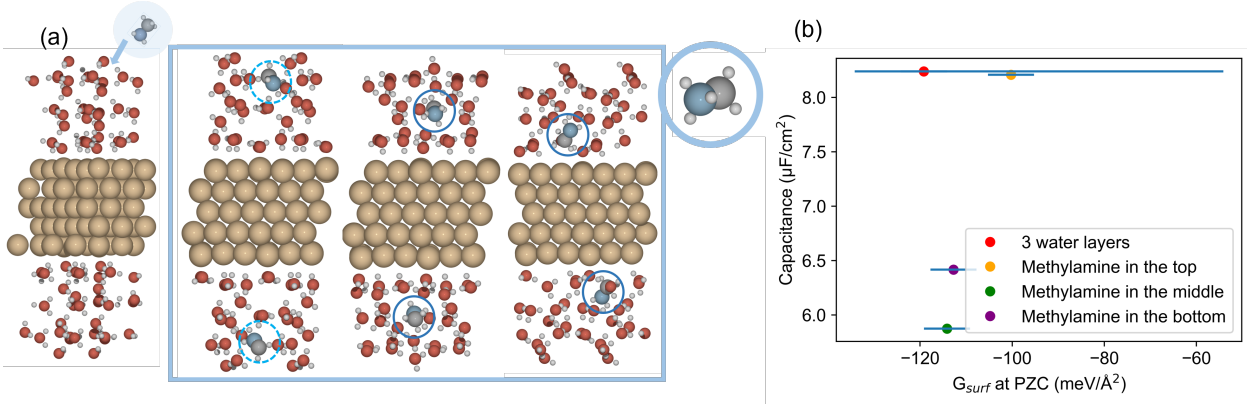

Figure 2.6: Diagram of mixture models where methylamine is in the top layer, middle layer and bottom layer with highlighted formation of $CH_3NH_3^+OH^-$ complex (blue circle) and quasi-formation (blue dashed circle); (b) capacitance calculated from the static approach and corresponding adsorption free energy per surface area for those models

Figure 2.8 gives information of AIMD sampling. It is interesting to notice that when methylamine on the surface (in the bottom layer) and near the surface (in the middle layer), their interactions with water molecules with respect to resulted dielectric constant are pretty comparable. There is still a switch between that at 300 K and room temperature that the average capacitance will increase slightly. Compared with that in static calculations, the sequence of capacitance value ordering is still the same. Similarly, two methylamines plus three water molecules and three methylamines plus two water molecules also lower the capacitance compared with three water layers no matter in which layer they are. AIMD sampling analysis of capacitance provide powerful evidence.

At the same time, this decrease in capacitance not only can be explained from conductivity increase, but also local electric field theory can serve as clues. In electrochemical reduction reactions, it is common that local alkalinity builds up before the reaction takes place. In other words, the higher pH, the lower electric field, the more likely reduction reactions happen . At the same time, there is a positive relationship between electric field and capacitance. It is reasonable to say that methylamine does tend to stay with water and

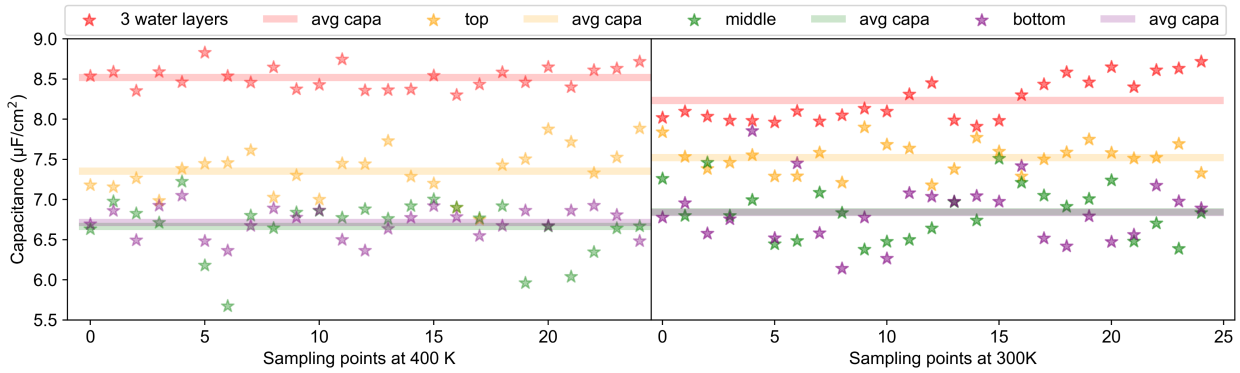

Figure 2.7: AIMD sampling of three water layers and mixture models of methylamine and water at 400K (left) and at 300K (right) at PZC including a snapshot every 200 steps during the second 5,000 steps of simulations, where their dynamic capacitance profiles are shown. The horizontal lines represent the average capacitance value.

result in hydrolysis.

2.5 Summary

In this work, theoretical calculations were applied to study the arrangement of the uncharged organic molecules acetone and methylamine in an aqueous solution at the potential of zero charge on or close to a copper electrode. Theoretical calculation displayed the same trends as observed in experiment and enables to give an explanation on a molecular basis. Through GCDFT calculations, the occurrence of a water depletion layer in the presence of hydrophobic acetone was calculated which causes significant dielectric effects and contributes to the increase in capacitance. For methylamine, however, a decrease in capacitance was calculated to be due to the -NH_2 group which causes an increase in the number of charged ions after hydrolysis. At the same time, AIMD serves as a powerful tool for sampling as many configuration spaces as possible to confirm the reason of capacitance change is coming from dielectric effects within water layers rather than fluctuations (etc., re-orientation) of water molecules. The microscopic picture of EDLs obtained in this work paves the way for a

better understanding of how uncharged organic molecules might arrange at electrode surface at the potential of zero charge.

CHAPTER 3

Dissolution of Copper electrode involving methylamine

This chapter is adapted from one unpublished paper: Y. Guan, J. Kümper, S. D. Mürtz, S. Kumari, P. J. C. Hausoul, R. Palkovits and P. Sautet, Origin of copper dissolution in electrocatalytic reduction conditions involving amines.

3.1 Background in Literature on Modelling of dissolution

In recent research, attention has been drawn to copper catalysts and their role in the electrochemical reduction of carbon dioxide (CO_2RR), which holds promise for sustainable energy conversion. Studies by Vavra et al.[26] have focused on elucidating the intermediates involved in driving copper catalyst rearrangement during CO_2RR. By employing advanced techniques such as online mass spectrometry (MS) and UV-visible absorption spectroscopy, their findings complement previous insights obtained through in situ electron microscopy, shedding light on a dissolution-redeposition process. Notably, transient species containing copper in the +1 oxidation state have been identified, with density functional theory offering insights into the formation of copper-adsorbate complexes in solution during catalytic operation. This investigation has identified copper carbonyls and oxalates as key species driving the reconstruction of copper surfaces during CO_2RR, underscoring the importance of understanding these mechanisms for improving catalyst stability and performance in practical applications.

Additionally, electrolysis, a fundamental process in electrochemistry, offers a platform

for visually observing the conversion of metal to its cation. Ikemoto et al.[27] have demonstrated this phenomenon using copper electrodes and a sodium polyacrylate electrolyte solution, providing valuable insights into the dissolution, migration, and deposition processes of copper ions during electrolysis. Such demonstrations serve as effective educational tools for conveying the principles of electrolysis to students at various academic levels. Moreover, the stability of copper-based electrocatalysts is paramount for their industrial applicability in CO_2 reduction processes. Speck et al.[28] investigated the corrosion behavior of copper across a range of pH conditions relevant to CO_2RR using an electrochemical on-line inductively coupled plasma mass spectrometer (ICP-MS). Their findings highlight significant copper dissolution in neutral and highly alkaline environments, while minimal dissolution occurs at intermediate pH levels. These results are instrumental in evaluating the stability and durability of copper-based electrocatalysts and guiding future research efforts aimed at enhancing their performance in CO_2 reduction applications.

3.2 Introduction

Copper electrocatalysts demonstrate high efficiency in facilitating electrochemical amination reactions[29, 6, 7, 30, 31] and numerous studies have shown that the arrangement of Cu surface atoms has a profound effect on performance [10, 11, 21]. Copper is also used for a large ensemble of electroreduction reactions, as CO and CO_2 electroreduction into C_1 and $C_2{}^+$ products[32, 33], where amines could be a co-reactant, for example in the case of the electroreduction of amine-captured CO_2. Even though several experimental instruments, such as liquid cell transmission electron microscopy (TEM) and in situ electron microscopy, can monitor the morphological evolution of electrocatalysts under reaction conditions, where the specific morphological features are responsible for a given activity and selectivity, the transient Cu-cation species in solution are straggling to be fully grasped since experimental conclusions are largely drawn from samples that have been removed from the electrochem-

ical environment and evaluated in the absence of an applied potential. However, these redox processes play a role in Cu-reconstruction, including dissolution and re-deposition . During the cell startup, when the working electrode experiences cathodic potentials, a dissolution–redeposition of Cu species in solution occurs and induces changes in the catalyst morphology and total exposed surface. This kind of changes is in need to be explored in order to design durable catalysts.

Here, after a 30 min electrolysis of an acetone/methylamine mixture, the concentration of Cu in the solution was measured, showing that at -0.75 V vs RHE, the concentration can still hold a value of around 13 ppm. To probe the underlying mechanism, grand canonical DFT was used to understand the reconstruction and dissolution of copper by complexation with soluble amine ligands. These ligands initially absorb on the Cu surface in electroreduction conditions and then enable transient restructuring and dissolution of Cu by forming coordination complexes with Cu cations. NH_3 is considered as a model amine in our calculations, but in addition ligand effects are explored by performing calculations for four other amines as ligands. Our study offers essential insights into the dynamic process of the Cu surface during electrochemical reduction, vital for designing durable Cu-based cathodes for a large array of processes.

3.3 Methods

Vienna ab initio simulation package (VASP) [34] as used to carry out all the periodic DFT calculations. The Perdew-Burke-Ernzerhof (PBE) parametrization of the generalized gradient approximation (GGA) of the exchange-correlation functional was employed, along with the dDsC dispersion correction to account for van der Waals interaction[35, 24]. The cut off energy is 400 eV. The interactions between the atomic cores and electrons were described by the projector augmented wave (PAW) method[36].

All structures were optimized under vacuum conditions first until the force and energy on

each atom was less than 0.01 eV / Å and 10^{-6} eV , respectively. Then geometry optimization based on implicit solvation provided by VASPsol was used to reach the force and energy on each atom was less than 0.05 eV / Å and 10^{-6} eV, respectively[25]. The Brillouin zone was sampled using 5 * 5 * 1 Gamma-centered k-point grids for structure optimization. The Gibbs free energies for adsorbates on the surface is obtained from the DFT energies with ZPE and entropy corrections determined from frequency calculations performed for all the considered structures using the harmonic oscillator approximation.

The grand canonical free energy was evaluated by grand canonical density functional theory (GCDFT) calculations, which is a surface charging technique[22]. Details can be found in our previous work. The linearized Poisson Boltzmann implicit solvation model implemented in VASPsol is used to represent the polarizable electrolyte region. The dielectric constant of water, 78.4, and the Debye screening length corresponding to 0.1 M concentration of electrolytes, 9.6 Å, were used. The surface slab is symmetrized along the z axis to avoid asymmetric potential in the implicit solvation region. Here the implicit solvent thickness is set to 60 Å for the symmetrized slab.

3.4 Results and Discussion

3.4.1 Restructuring and Dissolution Process on Kink Sites of Cu(843)

We use the Cu(843) surface to model low coordination defects present on the Cu electrode, as steps or kinks (Figure 3.1). The adsorption of methylamine or NH_3 on the kink sites, that possesses metallic coordination of 6 instead of 9 for the dense Cu(111) terrace, is significantly stronger than that on the (111) terrace (by about 0.5 eV, although the difference is potential dependent) (Figure 3.1), while the step site is intermediate. Considering the methylamine is interacting with the surface through an occupied lone pair orbital on N, injecting electrons at the surface by going to a more negative potential destabilizes the adsorption, which becomes endergonic for a potential more negative than -2 V vs RHE. Our

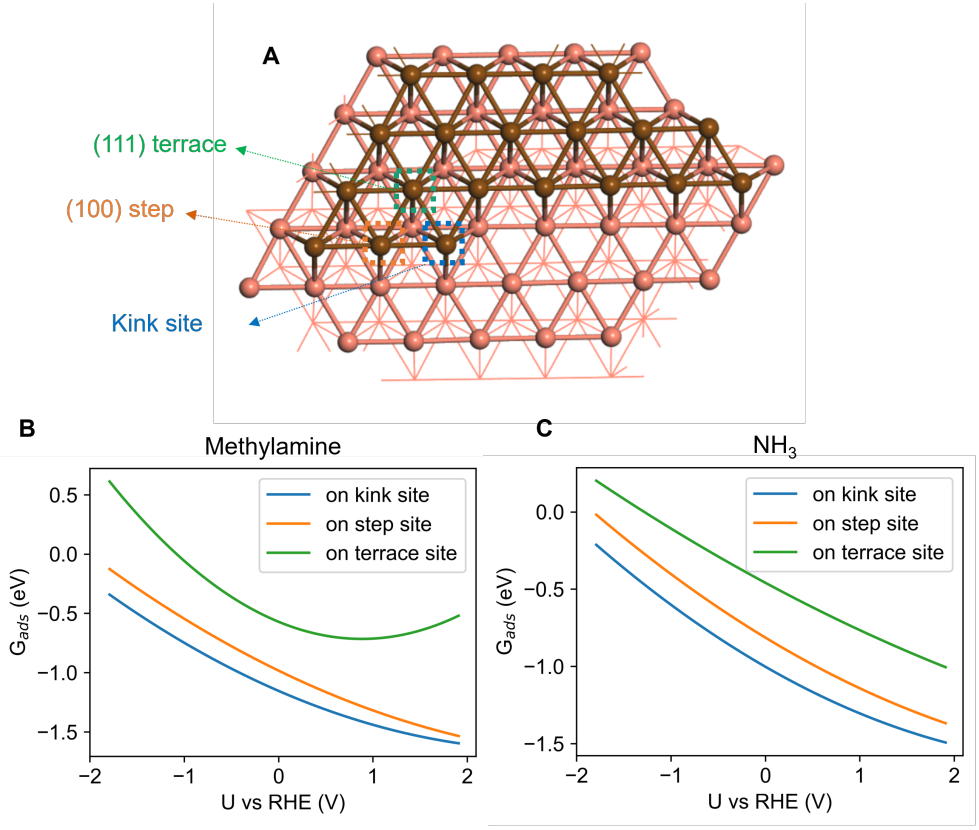

Figure 3.1: A) Three different adsorption sites on Cu (843), including kink site (1), (100) step (2) site and (111) terrace site (3). Free energy of adsorption of methylamine (B) or NH_3 (C) on the three different sites of Cu(843) as a function of potential.

starting model amine, NH_3, provides a similar adsorption energy compared to methylamine.

The stronger adsorption of NH_3 makes the kink site a good candidate for the dissolution process and mechanism. We start with one NH_3 molecule adsorbed on the kink site (Figure 3.2 structure 1a). We were not able to locate a stable configuration with two NH_3 molecules bound to the kink atom. However, upon one NH_3 adsorption, the kink Cu atom can be displaced on the terrace as an adatom with low metallic coordination of 3 (Figure 3.2 structure 1b). The energy required to form that NH_3 capped adatom is low (+0.1 to +0.3 eV depending on the potential, Figure 3.2 (c)), and this process creates a new kink atom, previously a neighbor of the former kink site. In addition, the formed Cu adatom can be

stabilized by the adsorption of a second NH_3, if the potential is less negative than -0.7 V vs RHE (Figure 3.2 structure 2). A third NH_3 can bind forming a pseudo-threefold $Cu(NH_3)3$ surface complex (Figure 3.2 structure 3). The binding of the fourth NH_3 is more difficult and adopts a "butterfly" C2v geometry (Figure 3.2 structure 4a). The surface complex can finally be detached to form a Cu^{2+} complex in solution, in a stabilizing process (Figure 3.2 structure 4b). The overall free energy profile for complexation and detachment depends on the potential. At positive (+0.5 V vs RHE) or zero potential the process is very easy and thermodynamically limited by the formation of the NH_3 capped Cu adatom. At negative potential, the process becomes limited by the formation of the $Cu(NH_3)_4$ surface complex. At -0.7 V vs RHE the formation of that surface $Cu(NH_3)_4$ complex represents a reasonable thermodynamic barrier of 0.51 eV. It can be underlined that forming the four-ligand surface complex $Cu(NH_3)_4$ is not mandatory, since starting from the surface $Cu(NH_3)_3$ complex, the approach of the fourth NH_3 can be concerted with the detachment of the complex. In that case, the thermodynamic barrier is only 0.21 eV at -0.7 V vs RHE. For a potential more negative than -0.7 V vs RHE, the calculations show that the dissolution process is not thermodynamically favored, and NH_3 adsorption on the kink site becomes more favorable than formation and detachment of the complex. This is clearly seen on Figure 3.2 (B), which represents the free energy of the various intermediates as a function of the potential. The main crossing point is at -0.7 V vs RHE. For more positive potential the dissolved Cu complex is more stable, while at more negative potential, the chemisorbed NH_3 is more stable. We assume here that the various processes have low activation energy, which is typically the case for adsorption and metal atom diffusion at metal surfaces. The dissolution of the kink Cu atom generates a new kink atom on the surface, and the process can continue. At pH 12, the Pourbaix diagram of Cu water shows the formation of $Cu(OH)_2$ at a potential more positive than +0.4 vs RHE, while the Cu surface is stable at more negative potentials. Our simulations show the formation of OH adsorbates on the Cu(843) surface at potential more positive than 0.25 V vs RHE. The presence of NH_3 therefore results in a considerable shift

in potential of the stability domain of the Cu electrode, favoring dissolution by formation of the $Cu(NH_3)_4$ dication until a potential of -0.7 V vs RHE. The implication is that Cu electrocatalysts cannot be used in a stable manner for electroreduction in the presence of amines.

3.4.2 Restructuring and Dissolution Process on the Cu(111) Surface

The dissolution process starting from a dense Cu(111) surface requires to extract a high coordination atom (coordination 9). We have explored two scenarios. These both start by adsorption of one NH_3 on the Cu(111) surface (Figure 3.3, 1a and Figure 3.4, 1a), which is slightly less stable than that on the Cu(843) kink. The second step extracts the surface atom to form a NH_3-capped adatom on the terrace (Figure 3.3, 1b and Figure 3.4, 1b). This forms a surface vacancy. In the first scenario, shown in the Supplementary Information Figure 3.4, the vacancy is kept as is and the process is highly endergonic (by + around 1.50 eV) making it unfavorable. As a second scenario, we suppose that one atom diffuses from the bulk in a concerted way and refills the vacancy. In this condition, the formation of the NH_3-capped adatom is only uphill by 0.24 eV at 0 V vs RHE , compared to 0.20 eV for the Cu(843) kink site . The formation of the surface Cu complex occurs in a similar way, with the coordination of a second, third and fourth NH_3 molecules, followed by the detachment of the tetra-coordinated Cu di-cation. The process is globally less favorable than on the kink atom of the Cu(843) surface. For example, at U=0 V vs RHE, the formation of the 4-coordinated surface complex (4a) is less stable by 0.39 eV compared to the initial adsorbed structure for one NH_3 molecule on the kink (1a), while it was slightly more stable for the kink site. The limited stability of the 4-coordinated surface complex can be also illustrated by the unusually long distance for two C-N bonds, 2.6 Å compared to 2.1 Å in the other cases. This reduced stability is explained by some lateral repulsion between NH_3 ligands and the flat Cu(111) surface, compared to the somewhat convex situation in the vicinity of the kink site.

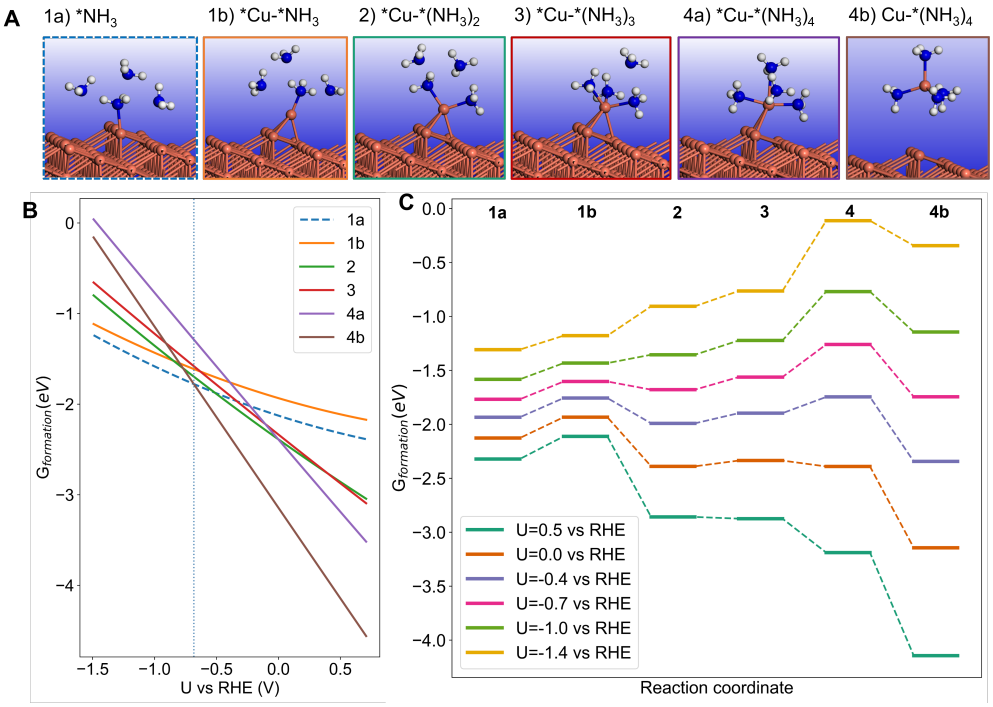

Figure 3.2: Dissolution of the Cu(843) surface in the presence of NH_3 in water as a function of the potential, initiated at the kink site. A) mechanisms and intermediates during the dissolution; 1a: adsorption of one NH_3 on the Cu kink site, 1b: diffusion of the NH_3-capped kink site Cu atom forming a Cu adatom on the nearby terrace; adsorption of a second (2), third (3) and fourth (4a) NH_3 on the formed Cu adatom; (4b) $Cu(NH_3)_4{}^{2+}$ di-cation formation and detachment. B) Free energy of the NH_3 induced surface or dissolved intermediates described in (A). The vertical blue dashed line describes the threshold potential above which the dissolved complex becomes most stable. C) Potential dependent reaction pathway for NH_3 adsorption, surface complex formation and detachment, where labels refer to (A).

The potential threshold for the stability of the dissolved Cu is -0.7 V vs RHE, exactly the same value as that for Cu(843). This is due to the fact that the binding energy of the kink atom on Cu(843) is equal to the binding energy of Cu in the bulk. In the case of the Cu(111) surface, if the vacancy is filled by a bulk atom, then the dissolution process is equivalent to the detachment of a bulk atom.

Therefore, the dissolution of an atom from a (111) terrace of Cu is possible, if we assume that the formed vacancy can be refilled in a concomitant way by a Cu atom from the bulk. It is somewhat less favorable, however, than the dissolution of a kink atom. In contrast, if the vacancy at the (111) surface is maintained, then the formation of the surface complex and its detachment become highly endergonic.

3.4.3 Analysis of the Cu Dissolution from a Chemical Bonding Perspective

The strength of the chemical bond between the formed Cu adatom and the surface along the surface complex formation can be estimated from the integrated Crystal Orbital Hamilton Population (-ICOHP) value, obtained from the one-electron band structure of the surface (Figure 3.5- A1 and B1). If we start from structure 1b, with one NH_3 ligand, we see that increasing the number of ligands leads to a weakening of the bond between the Cu atom of the surface complex and Cu atoms of the surface. The effect becomes especially strong if four NH_3 ligands are placed on the surface complex, with a reduction by about a factor of two for the case of the kink Cu(843) surface. The effect is similar to that on the (111) surface (in the hypothesis where one bulk atom diffuses and immediately fills the vacancy created by the extracted atom, even if the bond weakening is not as large). This decrease of the Cu-Cu bond strength by NH_3 adsorption is a key feature explaining the Cu atom extraction and dissolution. The driving force comes from the formation of Cu-N bonds via ligand bonding. Per Cu-N ICOHP is very comparable on (843) and (111) surfaces for 1, 2 or 3 ligands (1a, 1b, 2 and 3 structures), and the sum of ICOHP follows a very similar trend. However, when it comes to the fourth ligand binding (4a), the kink surface shows a better

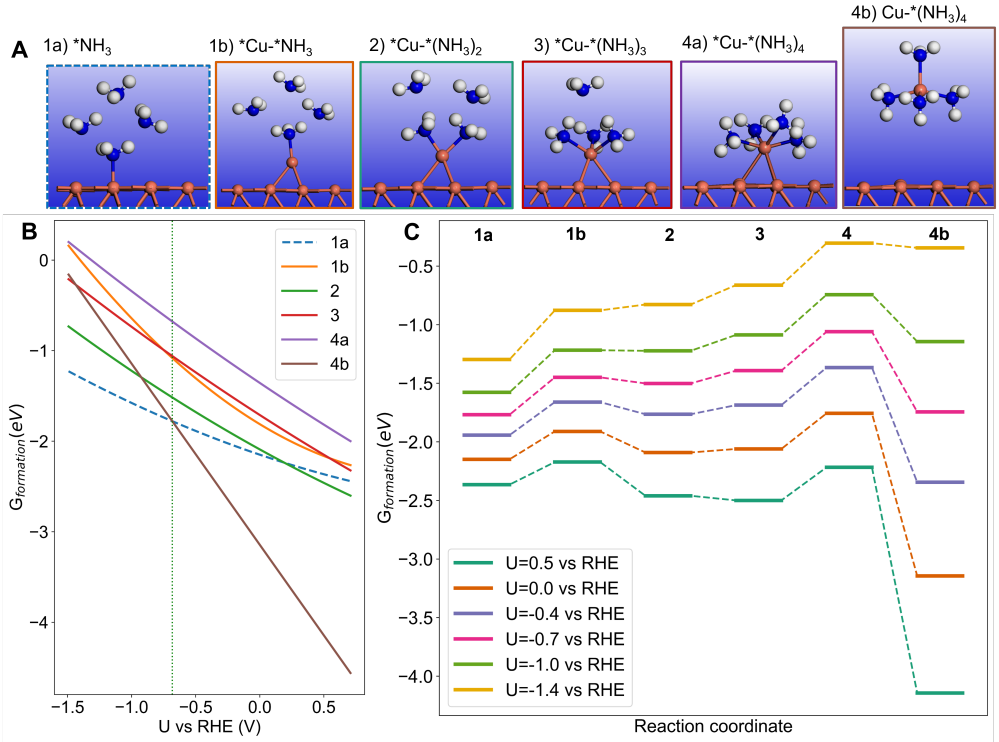

Figure 3.3: Dissolution of the Cu(111) surface in the presence of NH_3 in water, featuring the case where the vacancy is compensated by the concomitant migration of a Cu atom from the bulk, as a function of the potential. A) mechanisms and intermediates during the dissolution; 1a: adsorption of one NH_3 on the Cu surface, 1b: diffusion of the NH_3-capped Cu atom forming a Cu adatom on the surface, where the accompanying vacancy formation is compensated by the diffusion of a Cu atom from the bulk to the vacancy site; adsorption of a second (2), third (3) and fourth (4a) NH_3 on the formed Cu adatom; (4b) $Cu(NH_3)_4{}^{2+}$ di-cation formation and detachment. B) Free energy of the NH_3 induced surface or dissolved intermediates described in (A). The vertical blue dashed line describes the threshold potential above which the dissolved complex becomes most stable. C) Potential dependent reaction pathway for NH_3 adsorption, surface complex formation and detachment, where labels refer to (A).

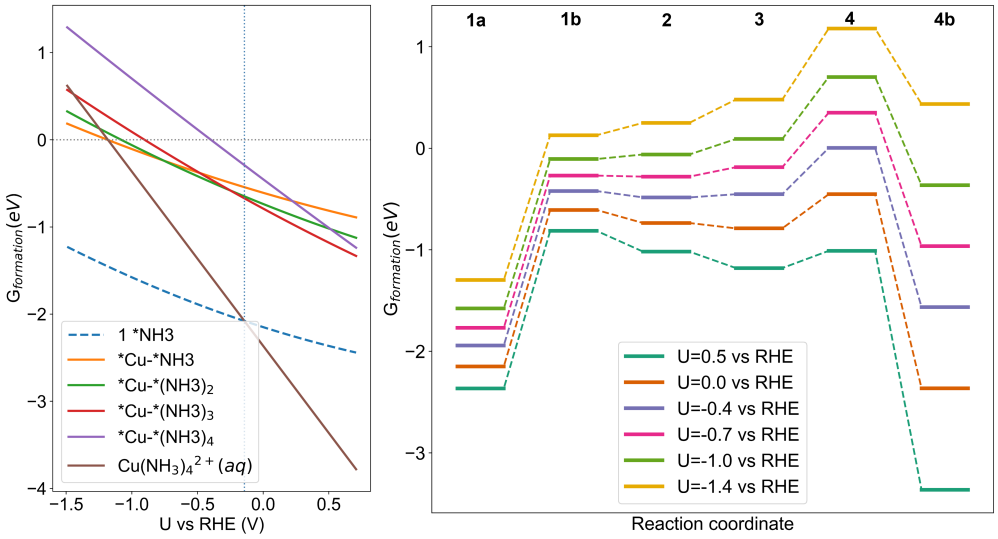

Figure 3.4: Dissolution of Cu surface and redeposition coupled with the formation of a vacancy on Cu(111) surface. The dashed lines show NH_3 initially covered surface with blue one for one NH_3 adsorption and orange one for two NH_3 adsorption. The solid lines represent the five dissolution and reposition stages, from dissolved Cu in the solution with ligands (pink line), to surface adsorbed Cu with four ligands (brown line), then to that with three ligands (purple), and then to that with two and one ligands. The pure adatom with four free ligands case is also considered in the study.

capacity to hold it, which is consistent with the higher summed -ICOHP between adatom Cu and surface Cu on Cu (843) and the better stability of the four-NH_3 surface complex.

3.4.4 Influence of the Nature of the Amine Ligand on the Dissolution Process

As discussed above, the NH_3 ligands enable the formation of a surface complex $Cu(NH_3)_n$ (n=1 to 4) that detaches as the $Cu(NH_3)_4$ di-cation. The ligands move the threshold potential for this Cu dissolution to a more negative value (-0.7 V vs RHE), compared to the case of water. Here we will discuss how this effect depends on the choice of the amine ligand. Four other ligands were checked, including methylamine, ethylamine, secondary dimethylamine and tertiary trimethylamine on the Cu(843) surface.

However, the stability of the intermediate surface Cu complexes does not follow the same trend. The initial extraction of the Cu kink atom with one ligand to form an amine-capped Cu adatom (from structure 1a to 1b) is slightly uphill in energy at 0V vs RHE for NH_3 and methylamine (0.22 eV and 0.24 eV resp.) and more difficult but still reasonable for other amines (ethylamine: 0.49 eV, dimethyl-amine: 0.24 eV, trimethyl-amine: 0.53 eV, Figure 3.6 C). The main difference is however in the formation of the surface complex with 2 and 3 ligands from 1b. The process is exothermic for NH_3, methylamine and ethylamine, while it is significantly endothermic for dimethyl-amine and trimethyl-amine. From the initial adsorbed amine (1a) the formation of the CuL_3 surface complex costs 0.83 and 0.96 eV in free energy for dimethyl-amine and trimethyl-amine, respectively. Calculations therefore show that the formation of the surface complex induces a thermodynamic barrier that cannot be passed at room temperature for dimethyl and trimethyl-amine even at U=0 V vs RHE. Changing the potential provides a consistent trend: the dissolution is easier at less negative potential, and always more difficult at more negative potential. This destabilization for the surface complex with two or three ligands comes from the bulky nature of these dimethyl and trimethyl-amines since ligands accumulated on the same Cu atom interact between them and/or with the surface. Therefore, the dissolution process can be kinetically controlled

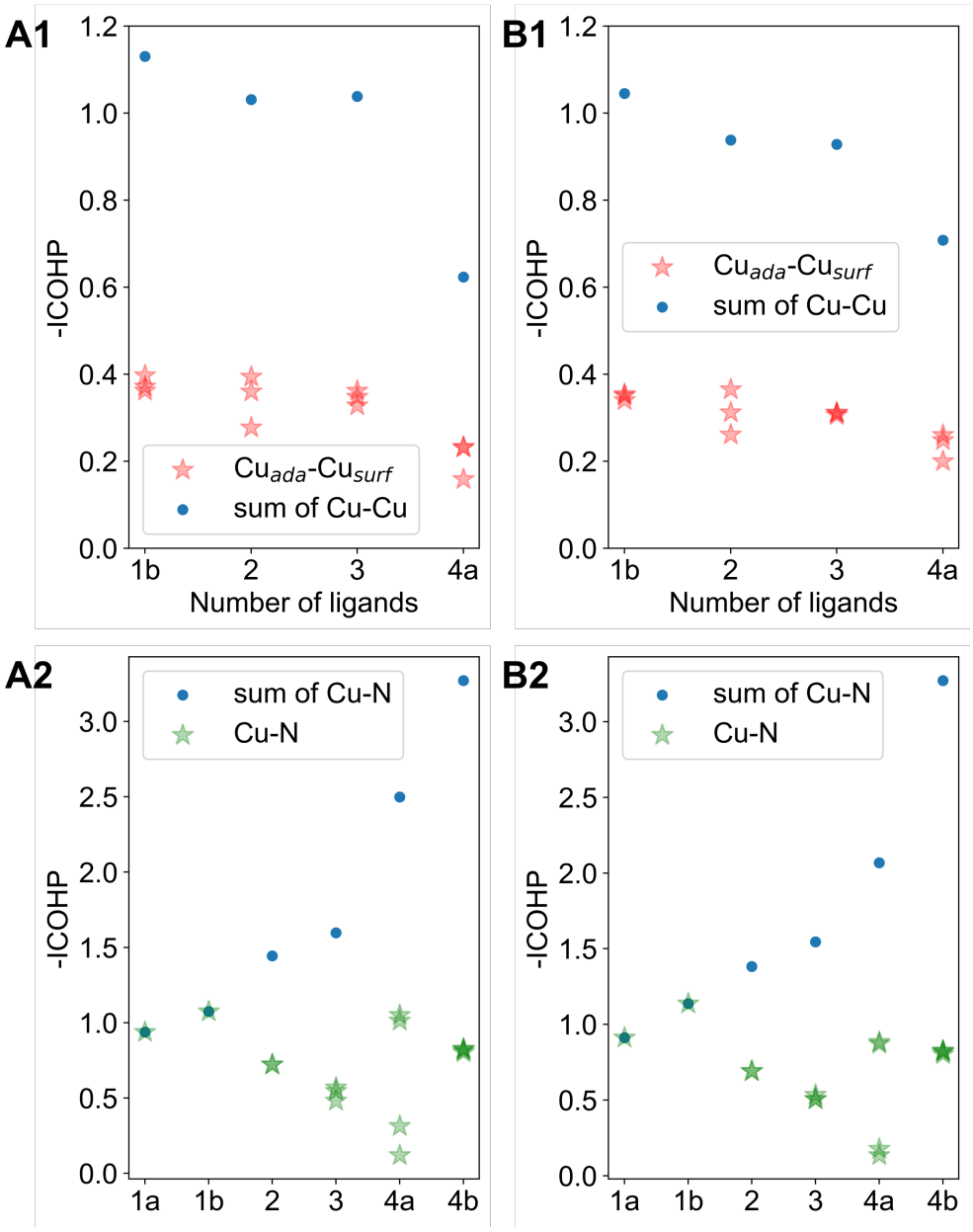

Figure 3.5: Chemical bond strength as quantified by the -ICOHP between extracted Cu in the surface complex and the three bonded surface Cu sites, as a function of the number of NH_3 ligands, on Cu(843) (A1) or Cu(111) (B1). Chemical bond strength as quantified by the ICOHP between extracted Cu in the surface complex and N atoms of the NH_3 ligands, as a function of the number of NH_3 ligands, on Cu(843) (A2) or Cu(111) (B2). Labels on the x axis refer to structures on Fig. 3.2 for Cu(843) and Fig. 3.3 for Cu(111).

by changing the bulkiness of the amine, where bulkier ligands are less prone to erode the surface. However, this secondary or tertiary amine cannot be used for the synthesis of secondary amines from carbonylic compounds in the considered amination reaction under alkaline conditions in water.

3.5 Summary

In complement to observations of dissolution of copper (Cu) and its negative impact on the performance of the reductive amination of acetone with methylamine as nitrogen source, even under reductive potential conditions (-0.75V vs RHE), this study employs Grand Canonical density functional theory to delve into this dynamic phenomenon from a microscopic perspective. The findings illustrate that amine ligands in solution directly adsorb onto the electrode, coordinating with the metal center and driving surface rearrangement by moving Cu atoms into low coordination adatom positions. Subsequently, other ligands stabilize the formed copper-ligands complex on the Cu surface, eventually leading to the detachment of a Cu-tetramine dication complex in solution, even under negative potential conditions. Calculations indicate that dissolution is predicted to occur at a potential of -0.7 V vs RHE or higher. Besides, the electron-donating group in the ligands will contribute to the thermal stability of the complex, but amines with multiple substituent (secondary or tertiary) will hinder the possibility of formation of the surface complex from steric repulsion. The detachment of the Cu atom is facilitated by the weakening of the Cu-Cu bond, itself promoted by the multiple coordination of maine ligands on the Cu adatom. This work significantly advances our fundamental understanding of Cu dissolution facilitated by surface restructuring in amine solutions under electroreduction conditions. Such insights are crucial for the rational design of durable Cu-based cathodes for electrochemical amination and other amine-involving reduction processes.

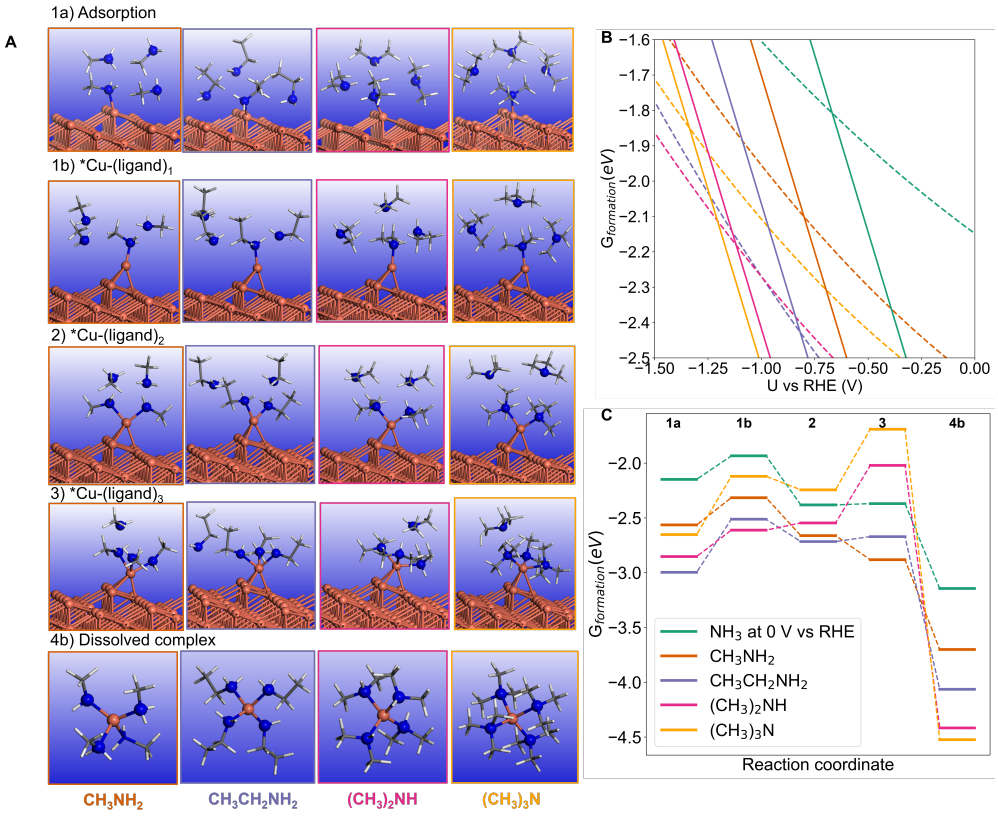

Figure 3.6: Influence of the type of amines on the structure and energy of the intermediate surface complexes on Cu(843) and of the dissolved di-cation, using four amines as ligands, including methylamine, ethylamine, dimethyl-amine and trimethyl-amine from left to right . A) structure for the adatom with one ligand (1b), with two ligands (2), three ligands (3) and the corresponding detached complex (4b). B) energy diagram comparing ligand adsorption on the kink atom (structure 1a, dashed lines) and dissolved complex (4b, solid lines) for the five considered ligands: NH_3 (green), methylamine (orange), ethylamine (purple), dimethyl-amine (pink), trimethyl-amine (yellow). C) Free energy profile at 0 V vs RHE for each ligand for the adsorption of one ligand on the kink atom of Cu(843) (1a), the formation of the surface complex with one ligand (1b), two ligands (2), three ligands (3), and finally the detached di-cation CuL4 complex (4)

CHAPTER 4

Conclusion

Theoretical calculations shed light on the spatial arrangement of uncharged organic molecules, acetone, and methylamine, at the copper electrode-water interface. The presence of acetone induces a water depletion layer, causing significant dielectric effects and consequently increasing capacitance, while methylamine's -NH_2 group contributes to hydrolysis. Advanced molecular dynamics simulations further corroborate these findings, emphasizing the role of dielectric effects within water layers in modulating electrode-double layer interactions.

This integrated approach advances our fundamental understanding of the intricate mechanisms underlying Cu dissolution and organic molecule behavior at electrode interfaces, crucial for the rational design of durable Cu-based cathodes for electrochemical transformations. By bridging macroscopic observations with microscopic insights, this work provides a nuanced understanding of electrochemical processes, paving the way for the development of efficient and sustainable electrochemical methodologies.

In parallel, combining the observations on copper dissolution and its impact on reductive amination with the theoretical calculations elucidating molecular arrangements at the electrode surface, this study offers a comprehensive understanding of the dynamic interplay between metal dissolution and organic molecule behavior under electrochemical conditions.

The findings reveal that amine ligands play a pivotal role in mediating surface restructuring by directly coordinating with the copper electrode, leading to the rearrangement of surface atoms and subsequent detachment of copper ions into the solution. This dissolution

process, initiated at relatively negative potentials, is facilitated by the destabilization of Cu-Cu bonds and the formation of stable copper-ligand complexes on the surface. Moreover, the study highlights the influence of ligand structure, with electron-donating groups enhancing complex stability while steric hindrance from multiple substituents attenuates surface complex formation.

Bibliography

[1] M. Jitaru, D. A. Lowy, M. Toma, B. C. Toma, and L. Oniciu. Electrochemical reduction of carbon dioxide on flat metallic cathodes. 27(8):875–889.

[2] Yoshio Hori, Ryutaro Takahashi, Yuzuru Yoshinami, and Akira Murata. Electrochemical reduction of CO at a copper electrode. 101(36):7075–7081. Publisher: American Chemical Society.

[3] Erin T. Martin, Caitlyn M. McGuire, Mohammad S. Mubarak, and Dennis G. Peters. Electroreductive remediation of halogenated environmental pollutants. 116(24):15198–15234. Publisher: American Chemical Society.

[4] Tapas Kuila, Ananta Kumar Mishra, Partha Khanra, Nam Hoon Kim, and Joong Hee Lee. Recent advances in the efficient reduction of graphene oxide and its application as energy storage electrode materials. 5(1):52–71. Publisher: Royal Society of Chemistry.

[5] John J. Roylance and Kyoung-Shin Choi. Electrochemical reductive amination of furfural-based biomass intermediates. 18(20):5412–5417. Publisher: The Royal Society of Chemistry.

[6] Qi-Liang Yang, Xiang-Yang Wang, Jia-Yan Lu, Li-Pu Zhang, Ping Fang, and Tian-Sheng Mei. Copper-catalyzed electrochemical c–h amination of arenes with secondary amines. 140(36):11487–11494. Publisher: American Chemical Society.

[7] Xiang Yang, Qi-Liang Yang, Xiang-Yang Wang, Hao-Han Xu, Tian-Sheng Mei, Yan Huang, and Ping Fang. Copper-catalyzed electrochemical selective bromination of 8-aminoquinoline amide using NH4br as the brominating reagent. 85(5):3497–3507. Publisher: American Chemical Society.

[8] Baran Eren, Danylo Zherebetskyy, Laerte L. Patera, Cheng Hao Wu, Hendrik Bluhm, Cristina Africh, Lin-Wang Wang, Gabor A. Somorjai, and Miquel Salmeron. Activation of cu(111) surface by decomposition into nanoclusters driven by CO adsorption. 351(6272):475–478.

[9] Baran Eren, Robert S. Weatherup, Nikos Liakakos, Gabor A. Somorjai, and Miquel Salmeron. Dissociative carbon dioxide adsorption and morphological changes on cu(100) and cu(111) at ambient pressures. 138(26):8207–8211.

[10] Dongfang Cheng, Anastassia N. Alexandrova, and Philippe Sautet. H-induced restructuring on cu(111) triggers CO electroreduction in an acidic electrolyte. pages 1056–1061. Publisher: American Chemical Society.

[11] Dongfang Cheng, Ziyang Wei, Zisheng Zhang, Peter Broekmann, Anastassia N. Alexandrova, and Philippe Sautet. Restructuring and activation of cu(111) under electrocatalytic reduction conditions. 135(20):e202218575. _eprint: https://onlinelibrary.wiley.com/doi/pdf/10.1002/ange.202218575.

[12] Douglas Henderson and Dezső Boda. Insights from theory and simulation on the electrical double layer. 11(20):3822.

[13] Gloria Namibia Moraila-Martínez, Jonathan Josué Elisea-Espinoza, Enrique González-Tovar, and Guillermo Iván Guerrero-García. Concentrated aqueous solutions of multivalent macroions enhance the electrical double layer capacitance and differential capacitance of a planar supercapacitor. 400:124405.

[14] G.M. Essert, J.P. De Souza, S.P. Schwaminger, M.Z. Bazant, and S. Berensmeier. Understanding electrostatic interaction on strong cation-exchanger via co-ion valency effects. 342:126860.

[15] Stanislav V. Vassilev, David Baxter, Lars K. Andersen, and Christina G. Vassileva. An overview of the chemical composition of biomass. 89(5):913–933.

[16] John J. Roylance and Kyoung-Shin Choi. Electrochemical reductive amination of furfural-based biomass intermediates. 18(20):5412–5417. Publisher: The Royal Society of Chemistry.

[17] Yinon M. Bar-On, Rob Phillips, and Ron Milo. The biomass distribution on earth. 115(25):6506–6511. Publisher: Proceedings of the National Academy of Sciences.

[18] Lang Li. Unraveling molecular structures and ion effects of electric double layers at metal water interfaces.

[19] Matteo Gentile, Sebastiano Bellani, Marilena I. Zappia, Agnese Gamberini, Valentina Mastronardi, Matteo Abruzzese, Luca Gabatel, Lea Pasquale, Sergio Marras, Ahmad Bagheri, Hossein Beydaghi, Evie L. Papadopoulou, Guglielmo Lanzani, and Francesco Bonaccorso. Hydrogen-assisted thermal treatment of electrode materials for electrochemical double-layer capacitors. Publisher: American Chemical Society.

[20] Kendra Letchworth-Weaver and T. A. Arias. Joint density functional theory of the electrode-electrolyte interface: Application to fixed electrode potentials, interfacial capacitances, and potentials of zero charge. 86(7):075140. Publisher: American Physical Society.

[21] Zisheng Zhang, Jun Li, and Yang-Gang Wang. Modeling interfacial dynamics on single atom electrocatalysts: Explicit solvation and potential dependence. 57(2):198–207. Publisher: American Chemical Society.

[22] Stephan N. Steinmann and Carine Michel. How to gain atomistic insights on reactions at the water/solid interface? 12(11):6294–6301. Publisher: American Chemical Society.

[23] Kiran Mathew, V. S. Chaitanya Kolluru, Srinidhi Mula, Stephan N. Steinmann, and Richard G. Hennig. Implicit self-consistent electrolyte model in plane-wave density-functional theory. 151(23):234101.

[24] Sarah Gautier, Stephan N. Steinmann, Carine Michel, Paul Fleurat-Lessard, and Philippe Sautet. Molecular adsorption at pt(111). how accurate are DFT functionals? 17(43):28921–28930.

[25] Kiran Mathew, Ravishankar Sundararaman, Kendra Letchworth-Weaver, T. A. Arias, and Richard G. Hennig. Implicit solvation model for density-functional study of nanocrystal surfaces and reaction pathways. 140(8):084106.

[26] Jan Vavra, Gaétan P. L. Ramona, Federico Dattila, Attila Kormányos, Tatiana Priamushko, Petru P. Albertini, Anna Loiudice, Serhiy Cherevko, Núria Lopéz, and Raffaella Buonsanti. Solution-based cu+ transient species mediate the reconstruction of copper electrocatalysts for CO2 reduction. pages 1–9. Publisher: Nature Publishing Group.

[27] Isao Ikemoto and Kouichi Saitou. Visual observation of dissolution of copper ions from a copper electrode. 90(6):763–764. Publisher: American Chemical Society.

[28] Florian D. Speck and Serhiy Cherevko. Electrochemical copper dissolution: A benchmark for stable CO2 reduction on copper electrocatalysts. 115:106739.

[29] Sonja D. Mürtz, Nils Kurig, F. Joschka Holzhäuser, and Regina Palkovits. Reviving electrocatalytic reductive amination: a sustainable route from biogenic levulinic acid to 1,5-dimethyl-2-pyrrolidone. 23(21):8428–8433. Publisher: The Royal Society of Chemistry.

[30] Titli Ghosh, Hazuki Kaizawa, Shohei Funato, M. Azadur Rahman, Norihiko Sasaki, Toshiki Nokami, Manabu Abe, and Takashi Nishikata. Formation of sterically congested cn bonds by electrochemical reductive coupling of amines and -bromocarboxamides. n/a:e202300636. _eprint: https://onlinelibrary.wiley.com/doi/pdf/10.1002/celc.202300636.

[31] Pim J. L. Broersen, Thijs. de Groot, Didjay F. Bruggeman, Emma S. Caarls, Jamie A. Trindell, Dimitra Anastasiadou, Marta C. Figueiredo, Gadi Rothen-

berg, and Amanda C. Garcia. Enhancing electrocatalytic synthesis of glycine with CuPb1ml electrode synthesized via pb UPD. 16(4):e202301370. _eprint: https://onlinelibrary.wiley.com/doi/pdf/10.1002/cctc.202301370.

[32] Runhua Chen, Xiaolong Zu, Juncheng Zhu, Yuan Zhao, Yuhuan Li, Zexun Hu, Shumin Wang, Minghui Fan, Shan Zhu, Hongjun Zhang, Bangjiao Ye, Yongfu Sun, and Yi Xie. Dynamically reconstructed triple-copper-vacancy associates confined in cu nanowires enabling high-rate and selective CO2 electroreduction to c2+ products. n/a:2314209. _eprint: https://onlinelibrary.wiley.com/doi/pdf/10.1002/adma.202314209.

[33] Panagiotis Trogadas, Linlin Xu, and Marc-Olivier Coppens. From biomimicking to bioinspired design of electrocatalysts for CO2 reduction to c1 products. 136(1):e202314446. _eprint: https://onlinelibrary.wiley.com/doi/pdf/10.1002/ange.202314446.

[34] G. Kresse and J. Furthmüller. Efficiency of ab-initio total energy calculations for metals and semiconductors using a plane-wave basis set. 6(1):15–50.

[35] John P. Perdew, Kieron Burke, and Matthias Ernzerhof. Generalized gradient approximation made simple. 77(18):3865–3868.

[36] G. Kresse and D. Joubert. From ultrasoft pseudopotentials to the projector augmented-wave method. 59(3):1758–1775.